ASIAN JOURNAL OF CIVIL ENGINEERING (BHRC) VOL. 16, NO. 6 (2015)
PAGES 803-817

THREE-DIMENSIONAL STRAIN ANALYSIS OF FLEXIBLE PAVEMENT STRUCTURES USING INFINITE ELEMENTS

Kh. Sandjak[1,2*] and B. Tiliouine[2]
[1]Faculté des sciences de l'ingénieur (F.S.I), Université M'hamed Bougara, Boumerdes, Algeria
[2]Ecole Nationale Polytechnique (E.N.P), Algiers, Algeria

Received: 7 February 2015; **Accepted:** 2 May 2015

ABSTRACT

This paper presents the main results of a numerical investigation on the three-dimensional (3-D) strain analysis of flexible pavement structures using a coupled Finite Element-Mapped Infinite Element (FE-MIE) model. The validation and numerical performance of this model are assessed by confronting critical pavement responses with Burmister's solution and FEM simulation results for multi-layered elastic structures. The coupled model is then efficiently utilised to perform 3-D simulations of a typical flexible pavement structure in order to investigate the impact of two tire configurations (conventional dual and new generation wide-base tires) on critical pavement response parameters. The numerical results obtained show the effectiveness and the accuracy of the coupled FE-MIE model. In addition, the simulation results indicate that, compared with conventional dual tire assembly, single wide base tire caused slightly greater fatigue asphalt cracking and subgrade rutting potentials and can thus be utilised in view of its potential to provide numerous mechanical, economic and environmental benefits.

Keywords: Infinite elements; 3-D strain analysis; flexible pavements; dual and wide base tires.

1. INTRODUCTION

Transportation is considered to be one of the most important infrastructure components influencing production and economic activities of a country. In Algeria, presently, low to moderate traffic roads represent more than 80% of the national road network. These roads are generally represented by thinly surfaced asphalt layers with significant unbound granular base and subbase layers resting on semi-infinite subgrade soils.

Finite elements are widely used in the solution of many engineering problems with unbounded domains. Examples of civil engineering problems can be found in typical areas

*E-mail address of the corresponding author: khaled.sandjak@g.enp.edu.dz (Kh. Sandjak)

of fluid structure interaction [1], soil-structure interaction [2], geomechanics and pavement engineering [3,4]. Nevertheless, the main drawback of the Finite Element Method (FEM) is the use of large truncated meshes to model unbounded domains leading to uneconomical solutions [5]. As a matter of fact, its application for unbounded domains presents some difficulties related to boundary conditions and often requires the use of a large number of elements to closely represent the asymptotic behaviour in the far-field of the analysed system.

In the last three decades, the infinite element method has emerged as an alternative solution technique [6-10]. In this method, the near-field region is modelled by finite elements and the far-field region is modelled by infinite elements. In this context, the use of a coupled Finite Element-Mapped Infinite Element (FE-MIE) model may provide, as will be shown in this paper, accurate and computationally effective solutions.

3-D modelling is more appropriate, compared to the axi-symmetric or 2-D plane strain model particularly for the simulation of mechanical behaviour of pavements structures with complex materials properties, subjected to multiple wheel loads and more realistic tire loading configurations. In this study, the 3-D FE-MIE model was considered to allow for more accurate and economical solutions as well as more realistic tire configurations that were judged essential in order to accurately simulate pavement responses to truck loading [11-13].

In accordance with the Mechanistic-Empirical Pavement Design [14], critical pavement tensile strains at the bottom of the asphalt layer and compressive vertical strain on the top of the subgrade soil constitute key input parameters for pavement design and for the development of distress models in terms of bottom-up fatigue cracking [15] and subgrade rutting [16]. In this work, however, considering the limited accuracy and high variability of the parameters used in the currently available performance distress models, computed pavement ratios were used as indicator of pavement damage caused by the two studied tire configurations: conventional dual tire assembly and single wide base (SWB) tire.

This paper presents the main results of a numerical investigation on the 3-D strain analysis of flexible pavement structures using a coupled FE-MIE model. The numerical performance of the coupled model is assessed by confronting the computed critical pavement responses with both Burmister’s solution for multi-layered elastic structures and numerical solutions obtained by the finite element method. Furthermore, the engineering application of the coupled model is illustrated by efficiently performing the 3-D simulations of a typical flexible pavement structure in order to investigate the impact of two tire configurations (conventional dual and new generation SWB tires) on pavement response. Based on the simulation results, conclusions of engineering interest are also reported.

2. BACKGROUND ON INFINITE ELEMENT METHOD

The main objectives in developing infinite elements for the analysis of unbounded systems are to model the far field domain economically. Two approaches may be used in general: the decay function and the mapped infinite element techniques. A detailed description of these two approaches may be found in reference [10].

2.1 Decay function approach

The decay function approach used to derive an infinite element for the far field domain, starting from the 4–nodes linear isoparametric finite element, consists in extending the domain of definition of the natural co-ordinate outside the finite element up to infinity in the upstream direction. The interpolation functions F_i associated with node i, used for the infinite element represented in Fig. 1, are obtained by multiplying the ordinary finite element shape functions N_i by a descent function decaying asymptotically to zero toward infinity.

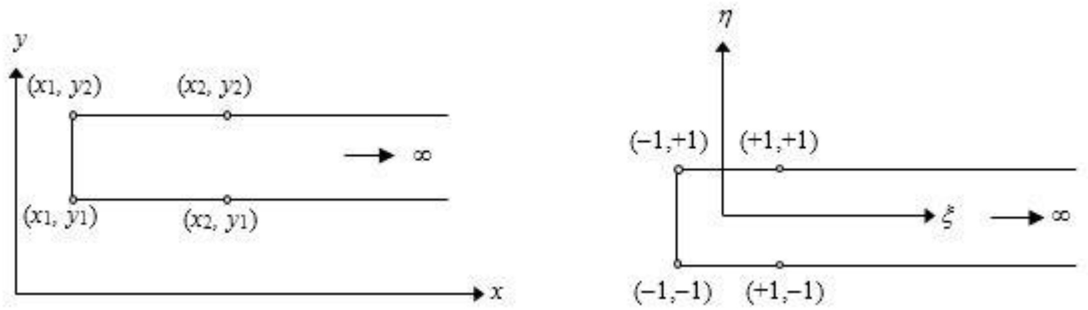

(a) physical coordinates (b) reference coordinates

Figure 1. Decay function infinite element in horizontal direction.

Fig. 1 shows that the field of physical coordinates and field reference coordinates are both infinite. The unknown variables are expressed in terms of functions down toward zero to infinity. Interpolation functions of the infinite element are given by the expression:

$$F_i(\xi,\eta) = N_i(\xi,\eta)\, h_i(\xi,\eta) \tag{1}$$

with:

$F_i(\xi,\eta)$: Interpolation function of the infinite element

$N_i(\xi,\eta)$: Standard finite element shape function

$h_i(\xi,\eta)$: Descent function

The role of the decay function is to ensure that the behaviour of the element is a good representation of the physical the problem. The decay function must be equal to unity in each node. Generally, two types of decay functions are used, the decay exponential functions or the decay rational functions.

The implementation of the decay function approach into existing standard finite element packages need some modifications. It consists essentially in setting up, for the infinite direction, Gauss-Laguerre or modified Gauss-Legendre abscissa and weights, and evaluating the new infinite element shape functions F_i as well as their derivatives.

2.2 Mapped infinite element approach

Contrarily to the decay function approach, the mapped infinite element approach restricts the domain of the natural co-ordinate to the element interior and keeps the standard shape functions N_i for the interpolation of the unknown variable but resorts to ascent shape functions with a singularity at the boundary nodes which sends the physical nodes to infinity. Thus, in reference to Fig. 3, the physical co-ordinates at x_2 are sent to infinity and the physical domain is mapped onto the parent finite element domain through the use of the ascent shape function in such a way that, at the singularity points ξ=1, the corresponding mapped coordinates x_2 tends to infinity.

This approach, due initially to Zienkiewicz [6], has the advantage that the original Gauss-Legendre integration abscissa and weights are retained. The only change needed to a finite element routine to make the element infinite, is a new computation of the Jacobian matrix. The element extends from the points x_1 to x_2, which are at infinity. This element is to be mapped onto the finite domain $-1 < \xi < +1$ as shown in Fig. 2.

For the two dimensional case, the element mapping function can be derived from the one-dimensional mapping function in the ξ direction and the usual Lagrange polynomial shape function in the η direction. This simply involves multiplying the finite shape function in the η direction by the infinite mapping function in the ξ direction. The Jacobian matrix and its inverse may then be computed from the following expression:

$$J = \begin{bmatrix} F_{,\xi} \\ F_{,\eta} \end{bmatrix} [X\ Y] \tag{2}$$

where X and Y are the nodal co-ordinates of the element and the derivatives $F_{,\xi}$ and $F_{,\eta}$ are given in Table 1 below:

Table 1: Mapped functions and derivatives used for the evaluation of the Jacobian matrix

Node	1	2	3	4
ξ	-1	+1	+1	-1
η	–1	–1	+1	+1
F	$(1-\eta)/(1-\xi)$	-	-	$(1+\eta/(1-\xi)$
$F_{,\xi}$	$(1-\eta)/(1-\xi)^2$	-	-	$(1+\eta/(1-\xi)^2$
$F_{,\eta}$	$-1/(1-\xi)$	-	-	$1/(1-\xi)$

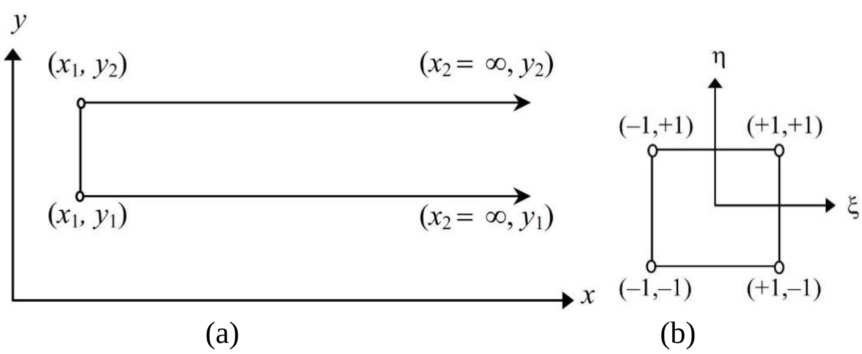

Figure 2. Mapped infinite element in the horizontal direction: (a) physical co-ordinates, (b) local co-ordinates

3. 3-D INFINITE ELEMENTS AND GEOMETRICAL MAPPINGS

In the three dimensional analysis, the pavement structure and subgrade soil in the near field region are modelled using the conventional 3-D 20 node brick elements as shown in Figs. 3 and 4. On the other hand, the far field region is divided into five kinds of regions which are respectively represented by horizontal, horizontal-corner, vertical, vertical-corner, and vertical–horizontal-corner infinite elements (HIE, HCIE,VIE, VCIE and VHCIE) as shown in Fig. 3. The nodal points in each infinite element are located on the interface with the finite element region. The number of nodes is eight for HIE and three for HCIE as indicated in Fig. 3(a). On the other hand, the number of nodes is eight, three and one for VIE, VCIE and VHCIE, respectively as in Fig. 3(b).

The mappings of the 3-D infinite elements from the global coordinates to the local coordinates are presented in Fig. 3 and for illustrative purposes in Table 2 for HIE.

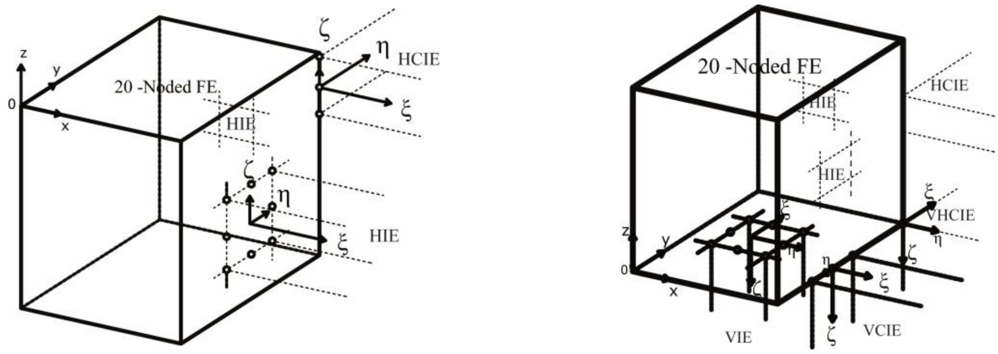

(a) (b)

Figure 3. Geometrical mappings: (a) Horizontal layered region; (b) Underlying half space

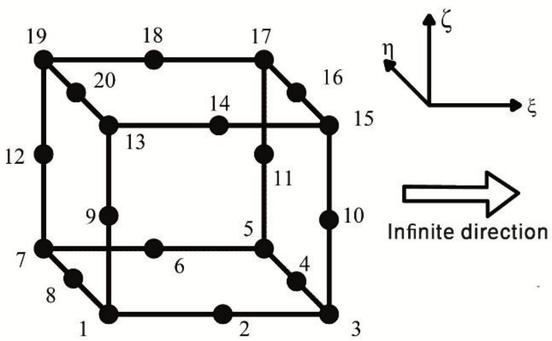

Figure 4. 20 node solid element (one infinite direction HIE)

Table 2: Geometrical transformation functions for HIE

Node i	M_i
1	-(1-η)(1-ζ)(2+ξ+η+ζ)/2(1-ξ)
2	(1+ξ)(1-η)(1-ζ)/4(1-ξ)
6	(1+ξ)(1+η)(1-ζ)/4(1-ξ)

7	-(1+η)(1-ζ)(2+ξ-η+ζ)/2(1-ξ)
8	(1-η)(1+η)(1-ζ)/(1-ξ)
9	(1-η)(1-ζ)(1+ζ)/(1-ξ)
12	(1+η)(1-ζ)(1+ζ)/(1-ξ)
13	(1-η)(1+ζ)(-2-ξ-η+ζ)/2(1-ξ)
14	(1+ξ)(1-η)(1+ζ)/4(1-ξ)
18	(1+ξ)(1+η)(1+ζ)/4(1-ξ)
19	(1+η)(1+ζ)(-2-ξ+η+ζ)/2(1-ξ)
20	(1-η)(1+η)(1+ζ)/(1-ξ)

The procedure for the formation of the stiffness matrix is as follows:
Form the Jacobian matrix, [J], with the relative mapping functions and their derivatives

$$[J] = \begin{bmatrix} \frac{\partial M}{\partial \xi} \\ \frac{\partial M}{\partial \eta} \\ \frac{\partial M}{\partial \zeta} \end{bmatrix} [X\ Y\ Z] \tag{3}$$

where X, Y and Z are nodal coordinate vectors of the element.
Invert $[J]$ to achieve $[J]^{-1}$
Use the parent finite element shape functions, N_i to obtain the matrix $[B]$

$$[B] = [J]^{-1} \begin{bmatrix} \frac{\partial N}{\partial \xi} \\ \frac{\partial N}{\partial \eta} \\ \frac{\partial N}{\partial \zeta} \end{bmatrix} \tag{4}$$

where $[B]$ is the matrix transforming the nodal displacements of the considered element to the Gaussian point strains within the element.
Form the stiffness matrix of the element

$$[K^e] = \iiint_{-1}^{+1} [B]^T\ [D][B]\ |J|\ \partial\xi\ \partial\eta\ \partial\zeta \tag{5}$$

Assemble the elementary stiffness matrices to form the global stiffness matrix $[K] = \sum^{N}[K^e]$; where N is the total number of elements.

4. VALIDATION AND PERFORMANCE OF THE COUPLED FE-MIE MODEL

The purpose of this section is to validate the proposed 3-D coupled model and illustrate its numerical performance. The classical problem of a uniformly loaded circular area on the surface of a multi-layered elastic structure (Burmister's problem) is used for this purpose. In what follows, the flexible pavement structure along with its geometrical and mechanical properties are first presented. The validation and numerical performance of the coupled model is then investigated in the next subsections.

4.1 Pavement structure and materials

The analysed structure comprises 6 cm of asphalt concrete (AC) layer, 20 cm of stiff unbound granular layer (UGM 1), 15 cm of unbound granular layer (UGM 2) and a theoretically semi-infinite subgrade soil (SS). This pavement structure typically represents thinly surfaced flexible pavements, with significant unbound granular layers, commonly used as pavement structures subjected to low to medium traffic volumes representing more than 80% of the road network in Algeria [17].

Data relative to the loading, the mechanical properties (i.e. resilient moduli E_i and Poisson ratios ν_i) of the constituent layers of the pavement structure and subgrade soil are shown in Fig. 5 [18].

A circular load of radius 0.175m and magnitude of 65 KN was applied to the pavement structure.

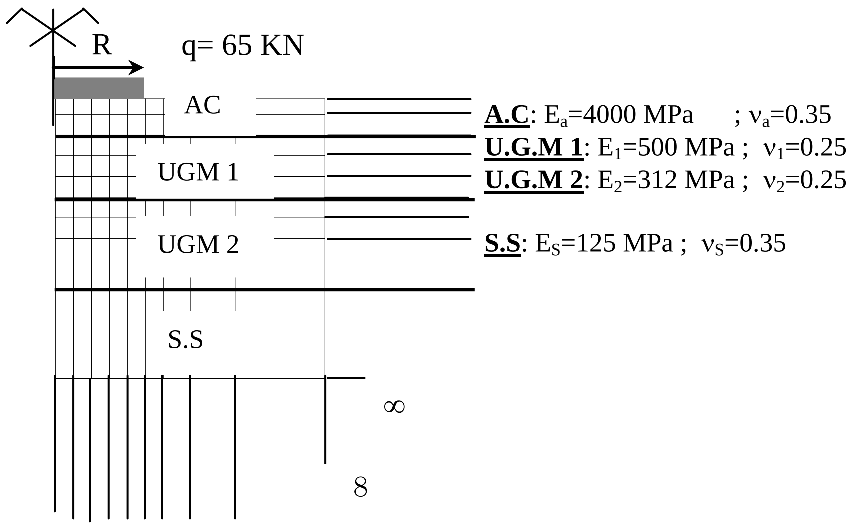

Figure 5. Pavement structure and mechanical properties of constitutive layers

4.2 Model validation and performance

Although utilizing infinite elements can eliminate the use of many finite elements in infinite domain, one still need to know where infinite elements should start.

A parametric study is performed herein to determine the optimal positions of infinite elements to be introduced either in both horizontal and vertical directions. The depth of examined pavement section was fixed to 20-times the radius R of loading area due to accurate subgrade responses. The investigated length of horizontal direction was varied from 10 to 20 R.

The main results of the numerical analyses are summarized in terms of values of the design criteria generally used in pavement engineering (see Table 3):

The horizontal tensile strain ε_{XX} at the bottom of the bituminous layer usually related to risks of asphalt layer cracking by tensile fatigue failure.

The vertical strain ε_{ZZ} at the top of the subgrade usually related to risks of rutting.

The deflection at the surface W, which is to some extent an indication of the structure ability to bear repeated traffic loads.

Table 3: Predicted critical pavement responses with infinite elements compared to multi-layered elastic solutions

Pavement response	Burmister's solutions	10R X20 R	15R X20 R	20R X20 R
W (mm)	0.595	0.581	0.588	0.592
ε_{XX} (micro)	148.00	148.06	147.73	147.68
ε_{YY} (micro)	-	118.45	118.20	118.14
ε_{ZZ} (micro)	638.00	630.24	631.80	631.93

It is observed from the results summarized in Table 3 that the longitudinal strain ε_{XX} is greater than the transverse strain ε_{YY} under wheel loading. This finding corroborates earlier experimental observations reported in previous experimental investigations [13]. Thus, in this work, the longitudinal strain ε_{XX} is selected as the critical strain response for bottom-up fatigue cracking of the asphalt layer.

Various solutions obtained using two truncated finite element models with coarse and fine meshes and the coupled FE-MIE model are confronted to solutions based on multi-layered elastic theory [16].

The first finite element model uses the mesh (A) with regular elements and includes10x10x10 elements (1000 finite elements) over 2x2 m in plane surface and 2 m in the vertical direction. The mesh (B) corresponds to a fine mesh (27306 elements) with dimensions of elements in geometric progression in both directions. The mesh (B) is applied to domain size of 140 times the radius of loaded area (R) in the vertical direction and 20 times R in horizontal direction.

The coupled model (mesh (C)) utilizes finite elements (6292 elements) coupled with five kinds of infinite elements (308 elements) the formulation of which, varies depending on their respective positions. Boundary conditions associated with meshes (A) and (B) are identical.

For illustrative purposes, the two truncated finite elements models, the coupled FE-MIE model and the corresponding meshes are presented in Fig. 6.

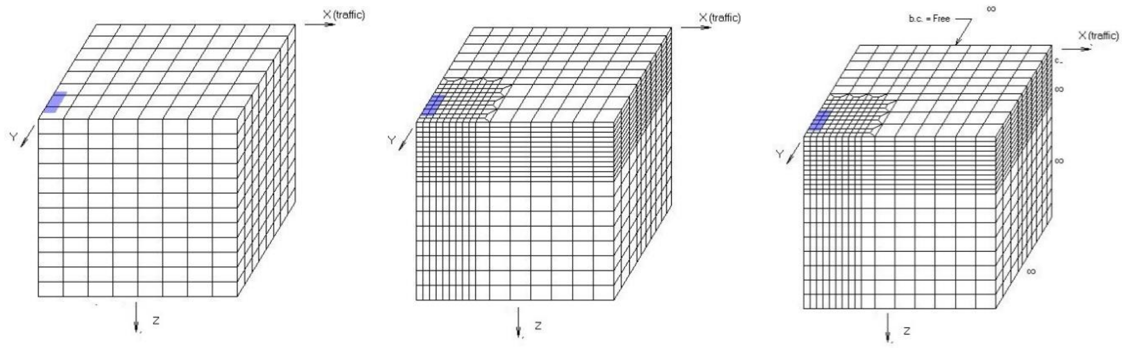

(a) Mesh (A) (b) Mesh (B) (c) Mesh (C)

Figure 6. Typical meshes used in this study: (a) Regular F.E; (b) Refined F.E; (c) FE-MIE

Simulation results obtained for the surface deflection using the two finite element models based respectively on coarse (Mesh A) and refined (Mesh B) and the coupled FE-MIE model (Mesh C), are presented in Table 4.

Table 4: Pavement surface deflections values for different FE and FE-MIE models

Surface deflection	Burmister's solutions	Mesh (A)	Mesh (B)	Mesh (C)
W (mm)	0.595	0.550	0.589	0.592

It is noted that the results obtained by the coupled model are very close to the results provided by Burmister's solution. It is also observed that the finite element model of mesh B gives good results while the results obtained by the model of mesh (A) are rather sketchy.

It is also noted that the coupled model provides better accuracy compared to the finite element model both in near field and far-field. In other words for the same level of accuracy, the gain achieved by using a mesh with infinite elements may be substantial. For the case considered here, this is a gain of around 77% in percentage of mesh elements and 80% in percentage of calculation time (see Table 5).

Table 5: Comparison of number of elements and CPU time between FE model and coupled model for 3D analysis

Nbre of elements and CPU time	FE model	Coupled model (FE-IF)	Gain (%)
Nbre of elements	27306	6320	76.85
CPU time (s)	383	79	79.37

These percentage gains in terms of CPU time will be greater in the case of non-linear pavement analysis.

5. 3-D PAVEMENT STRAIN ANALYSIS USING INFINITE ELEMENTS

The validated 3-D coupled model is now used to analyse a flexible pavement structure subjected to wheel loading with two tire configurations, conventional dual tire and SWB tire (Fig. 7) [13,19].

Figure 7. Single wide base and dual tires [20]

The new generation of SWB tire used since 2000, provide many advantages including improved fuel economy, lower wheel cost and reduced maintenance. Thus, the impact of the use of single wide base tire on pavement roads needs to be investigated. The dimensions of the two tire configurations are compared in Table 6.

Table 6: Tire configurations used in this study

Tire type	Overall diameter (mm)	Overall Width (mm)
315/80R22.5 (Dual)	1079	315
495/45R22.5 (SWB) *	1013	495

*495/45R22.5 define respectively the design width in millimeter, the aspect ratio (height/width) and inner diameter of wheel in inch.

3-D analysis pavement requires adequate modelling of the imprint shape. In this part of the study, a rectangular imprint shape is used for the two tire configurations. The contact area is taken equal to 94500 mm^2 and 74250 mm^2 for conventional dual and SWB tire respectively.

Table 7 below, summarizes the calculated longitudinal strain at the bottom of asphalt layer, the vertical strain at the top of subgrade and the ratios of SWB to the conventional dual tire strains.

Table 7: Simulation results

Tire type	Longitudinal Strain (micro)	Vertical Strain (mm)
Dual	333.487	523.420
SWB	358.544	597.688
Ratios	1.07	1.14

The investigation results presented in Table 7 show that, compared to the conventional dual-tire assembly, the wide-base 495 tire causes slightly greater longitudinal strain at the bottom of asphalt layer and vertical strain at the top of subgrade soil. These results also suggest the need to conduct future studies in order to further assess the impact of using SWB tire in view of its potential benefits such as improved fuel economy, lower wheel cost and reduced maintenance.

Figs. 8 and 9 compare the horizontal strain and vertical strain for the analysed pavement structure under both conventional dual assembly and SWB tire. Compared with the dual tire assembly, SWB tire induces 7% greater tensile strain at the bottom of asphalt layer and 14% greater compressive vertical strain at the top of subgrade soil. These findings indicate that the SWB tire could cause slightly more fatigue asphalt cracking and subgrade rutting potentials. Observed discontinuities in the variations of the longitudinal and vertical strains at the successive layer interfaces are due to corresponding changes in layer stiffness.

From the plots reported in Figs. 8 and 9, the impact of SWB tire compared to conventional dual assembly is essentially confined to Asphalt Concrete and Unbound Granular Materials layers. It is also seen that this impact becomes less significant as the depth increases because surface contact stress become less influential.

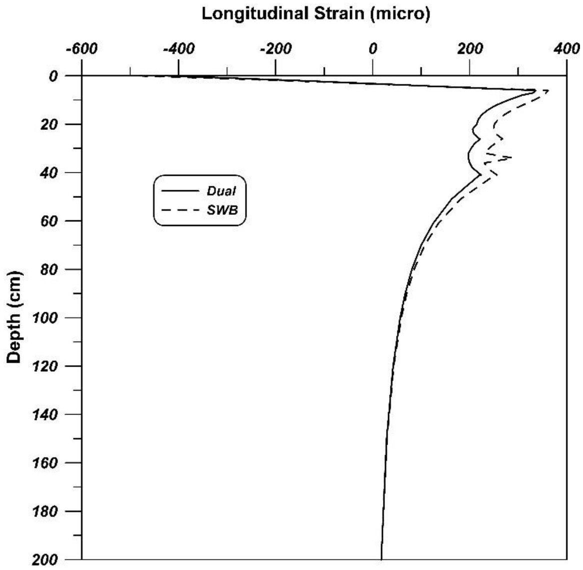

Figure 8. Variation of the longitudinal strain (ε_{XX}) with depth

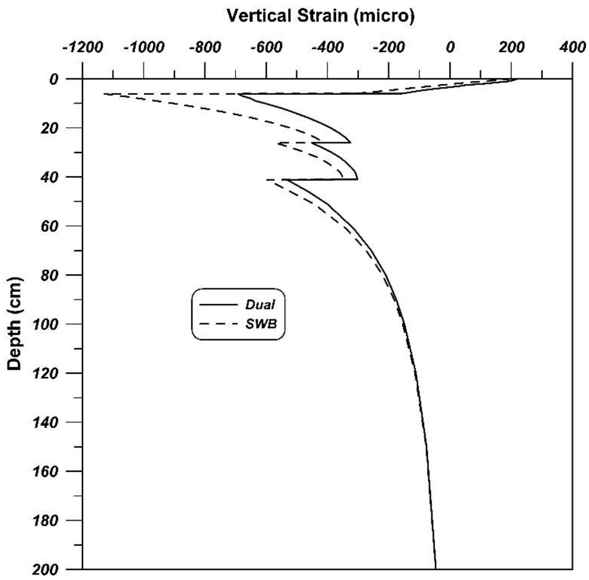

Figure 9. Variation of the vertical strain (ε_{ZZ}) with depth

For illustration purposes, contour plots throughout depth for vertical displacement (Fig. 10) and contours of tensile horizontal strain at the bottom of asphalt layer and compressive vertical strain at the top of subgrade soil are presented in Figs. 11-a and 11-b respectively.

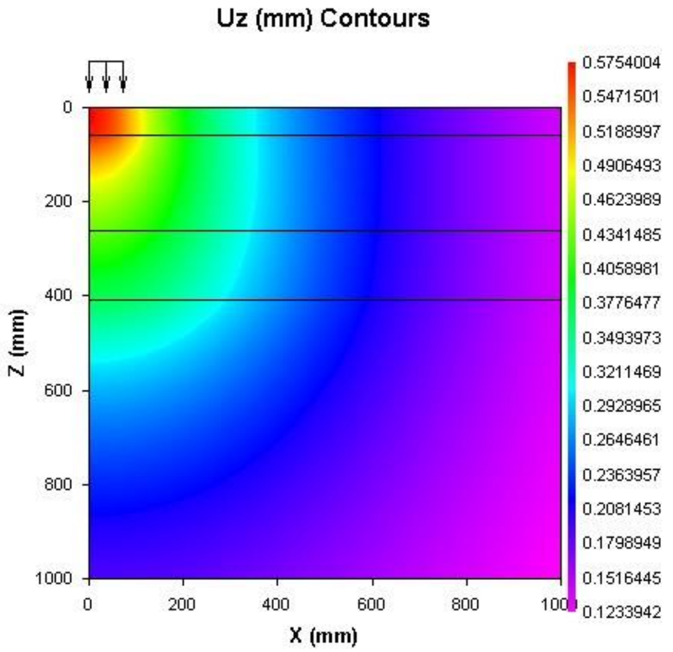

Figure 10. Contour plot of vertical displacement

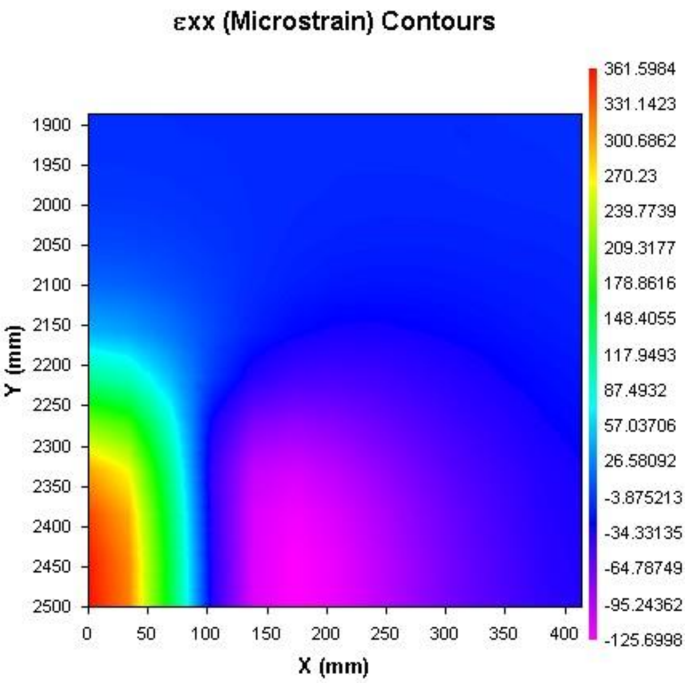

Figure 11a. Tensile strain at a bottom of asphalt layer

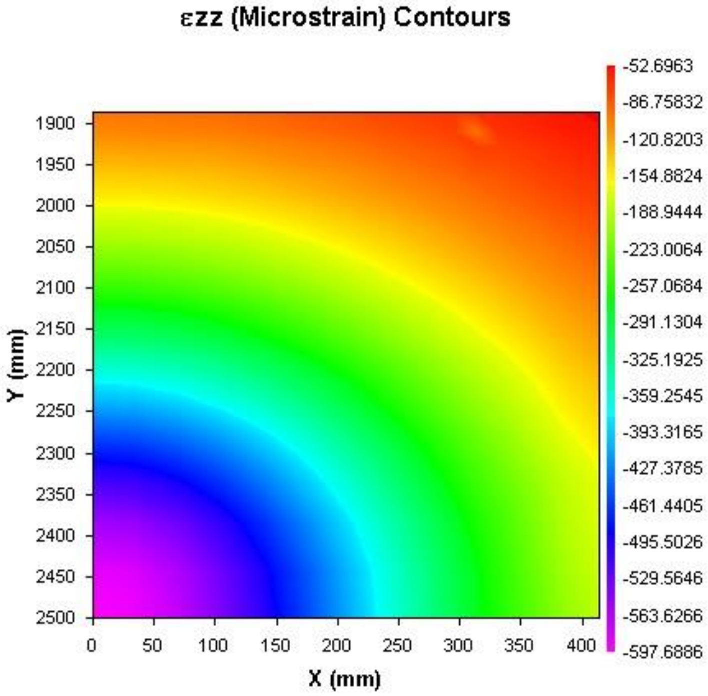

Figure 11b. Compressive vertical strain at the top of subgrade soil

From Fig. 10, it can be seen that the value of vertical displacement is maximum at the load axis and gradually decreases with depth and distance away from the loading axis. This observation remains valid for both cases of longitudinal tensile strains and vertical compressive strains as shown in Figs. 11(a) and 11(b).

6. CONCLUSIONS

In this paper, the main results of a numerical investigation on the 3-D strain analysis of flexible pavement structures using a coupled FE-MIE model are presented. An analytical framework is described, for presenting in a unified way two basic approaches to the infinite elements method. Furthermore, the functions of geometrical transformations necessary for the formulation of 3-D infinite elements based on the mapped infinite element approach are systematically generated in order to simulate the asymptotic behaviour in the far field of flexible pavement structures. The numerical performance of the coupled model is first assessed by confronting the computed critical pavement responses of a typical pavement structure subjected to low to moderate volume of traffic with Burmister's solution for multi-layered elastic structures and numerical solutions obtained by the finite element method. The coupled model is then utilised efficiently to perform the 3-D simulations of flexible pavements in order to investigate the impact of two tire configurations (conventional dual and new generation SWB tires) on critical pavement responses.

The mapped infinite element approach has the great advantage of keeping the same rule of standard numerical integration of Gauss-Legendre abscissae and weights frequently used in the finite element method which allows its implementation in a finite element program without major modification.

Results of the parametric study showed that, in order to achieve the similar level of accuracy with analytical solutions, the domain representing the near field (meshed with finite elements) needs to be 20 times the radius of loading area.

The accuracy of the coupled FE-MIE model is demonstrated by solving a problem of a uniformly loaded circular area on the surface of a multi-layered elastic structure. The simulation results show that the solutions obtained from the coupled numerical model are in excellent agreement with Burmister's solution. The simulation results show that for the same level of accuracy, the coupled numerical model enables a substantial gain compared to a truncated finite element model. For the case studied in this paper, this gain represents a percentage gain of 77% in number of elements and a similar percentage (about 80%) in CPU time, notwithstanding the saving in data file preparation time.

Moreover, the application of the numerical model for the 3-D strain analysis of a flexible pavement structure subjected to two tire configurations shows that, compared to the conventional dual-tire assembly, the SWB tire causes slightly greater longitudinal strain at the bottom of asphalt layer and vertical strain at the top of subgrade soil. These results also underline the need to perform future studies to further assess the impact of SWB tire on pavement by using a more general approach that considers mechanical, economic and environmental aspects.

REFERENCES

1. Mirzabozorg H, Kordzadeh A, Hariri-Ardebili MA. Seismic response of concrete arch dams including dam-reservoir- foundation interaction using infinite elements, *Electronic Journal of Structural Engineering*, No. 1, **12**(2012) 63-73.
2. Seo CG, Yun CB, Kim JM. Three-dimensional frequency-dependent infinite elements for soil-structure interaction, *Engineering Structures*, **29**(2007) 3106-20.
3. Patil VA, Sawant VA, Deb K. 3D finite-element dynamic analysis of rigid pavement using infinite elements, *International Journal of Geomechanics (ASCE)*, No. 5, **13**(2013) 533-44.
4. Luo H, Zhu HP, Miao Y, Chen CY. Simulation of top-down crack propagation in asphalt pavements, *Journal of Zhejiang University Science A*, **11(**2010) 223-30. [doi:10.1631/jzus.A0900248].
5. Houmat A. Mapped infinite p-element for two-dimensional problems of unbounded domains, *Computers and Geotechnics*, **35**(2008) 608-15.
6. Zienkiewicz OC, Bettess P, Chiam TC, Emson C. Numerical methods for unbounded field problems and a new infinite element formulation, *ASME, AMD*, **46**(1981) 115-48.
7. Beer G, Meek JL. Infinite domain elements, *International Journal for Numerical Methods in Engineering*, **17**(1981) 43-52.

8. Curnier A. A static infinite element, *International Journal for Numerical Methods in Engineering*, **19**(1983) 1479-88.
9. Marques JM, Owen DR. Infinite element in quasi-static materially non-linear problems, *Computers and Structures*, No. 4, **18**(1984) 739-51.
10. Bettess P, Betttess JA. Infinite elements for static problems, *Engineering Computations*, **1**(1984) 4-16.
11. Al-Qadi IL, Elseifi MA. New generation of wide-base tires: impact on trucking operations, environment, and pavements, *Journal of the Transportation Research Board*, **74**(2007) 100-9 [doi:10.3141/2008-13].
12. COST 334. Effects of wide single tyres and dual tyres, Final Report of the Action (Version 29), European Co-operation in the field of Scientific and Technical Research, 2001.
13. Grellet D, Doré G, Bilodeau JP. Comparative study on the impact of wide base tires and dual tires on the strains occurring within flexible pavements asphalt concrete surface course, *Canadian Journal of Civil Engineering - NRC Research Press*, **39**(2012) 526-35.
14. NCHRP Projet 1-37. A guide for mechanistic-empirical design for new and rehabilited pavement structures, Final report, Transportation Research Board, 2004.
15. Bosurgi G, Perlongo W. Numerical analysis of fatigue cracks growth in flexible pavements with the elastoplastic fracture mechanics method, *Structure and Infrastructure Engineering*, No. 8, **10**(2014) 1027-37.
16. Huang YH. *Pavement Design and Analysis*, Prentice Hall, Englewood Cliffs, USA, 2004.
17. Sandjak K, Tiliouine B. Experimental evaluation of non-linear resilient deformations of some algerian aggregates under cyclic loading, *Arabian Journal for Science and Engineering*, **39**(2014) 1507-16 [doi: 10.1007/s13369-013-0737-4].
18. Tiliouine B, Sandjak K, Ali-Haimoud CY. Effect of interface condition on performance of road pavement with non-linear granular materials, *Advanced Materials Research*, **587(**2012) 102-6 [doi: 10.4028/www.scientific.net].
19. Greene J, Toros U, Kim S, Byron T, Choubane B. Impact of wide-base single tires on pavement damage, *Journal of the Transportation Research Board*, No. 55, **21**(2010) 82-90.
20. Huft D. Research Related to Asphalt Pavements at the South Dakota Department of Transportation, *SD Asphalt Conference*, 2012.